13th World Conference on Earthquake Engineering
Vancouver, B.C., Canada
August 1-6, 2004
Paper No. 180

SEISMIC HAZARD MAPPING OF DELHI CITY

R.N.Iyengar[1] and S.Ghosh[2]

SUMMARY

Delhi the capital of India is a burgeoning metropolis having a population of some twelve million people. The city has experienced earthquakes in the past and is vulnerable for earthquake related damages in the future. There are nearby diffuse seismic sources known for their sporadic activity. In addition, the threat perception is highlighted by the proximity of the active Himalayan plate boundary region. Thus, seismic hazard at Delhi is controlled broadly by two different tectonic regimes namely, the Himalayan region (HR) and the Delhi region (DR). The present study aims at mapping the peak ground acceleration (PGA) values for Delhi city, using probabilistic seismic hazard analysis (PSHA) methods. Twenty potential faults, in a region of 300 km radius around Delhi, are identified. Recurrence relationships for the two controlling regions are established with the help of past (1720-2001A.D.) data. Regional attenuation relationship is developed using strong motion data recorded on rock sites. PSHA is performed for a 40km x 30km region encompassing Delhi and a microzonation map is prepared for PGA value, at a probability exceedance level of 2 percent in a period of 50 years, computed at 1200 grid points at 1km x 1km interval. Disaggregation of hazard in terms of magnitude and source to site distance has also been carried out. This shows that moderate local earthquakes contribute significantly, rather than the long distance Himalayan events, to the hazard in the city. The city has considerable variation in the soil layering and bed rock profile, which may cause large variation of surface level ground motion. Soil amplification studies are carried out at several representative sites to understand how the rock level PGA value gets altered at the surface level in the city.

INTRODUCTION

Delhi and its surrounding region have suffered earthquakes since ancient times. This has been highlighted in a series of papers by Chouhan [1], Srivastava and Roy [2] and Iyengar [3,4]. However, records of historical earthquakes start from 1720 A.D. only [3]. The Modified Mercalli Intensity (MMI) of this event has been estimated to be IX in the present Old Delhi area. A violent shock of MMI = IX is reported to have been felt near Mathura on 01.09.1803 [1]. A major earthquake took place near Bulandshahr on 10.10.1956. This event was felt over a large area with death and destruction [Verma, 5]. An earthquake known as Gurgaon earthquake of intensity VII occurred on 27.08.1960 near Sohna about 60 Km SE of Delhi, [Srivastava 6]. This event inflicted damage to property and about 50 persons were injured. An event of

[1]Professor, Dept. of Civil Engg., Institute of Science, Bangalore 560012, India.
Email: rni@civil.iisc.ernet.in
[2] Research Student, Indian Institute of Science, Email: susanta@civil.iisc.ernet.in

magnitude 4.0 was recorded on 28.07.1994. This was reported to have caused damage to the minarets of Jumma Masjid. On 28.02.2001 and 28.04.2001, Delhi experienced two small earthquakes of magnitude 4 and 3.8 respectively, of local origin. Far distance Himalayan earthquakes namely Kangra (04.04.1905) and Uttarkashi (19.10.1991) reportedly shook Delhi to the extent of intensities VI and V respectively. The felt intensity of the recent Chamoli (28.03.1999) earthquake was VI at Delhi, [IMD 7]. It is observed from the above discussion that Delhi gets affected by events originating locally as well as those from the Himalayan region. Thus, the control region around Delhi is inhomogeneous as far as its seismotectonics is concerned. The seismic zoning map of India, IS1893-2002, marks a fairly large region including Delhi to be in zone IV, specifying thereby the peak ground acceleration (PGA) for this region to be 0.24g. While this or another similar figure may be reasonable as a preliminary approximation for engineers to start with, earthquake resistant structural design will be successful to the extent the forces due to future shocks are accurately estimated at the site of a given structure. Earthquakes are low probability events but with very high levels of risk to the society. Hence, either under estimation or over estimation of the seismic hazard will prove costly in the long run. With the above points in view, an attempt is made here to prepare a microzonation map of Delhi city and its surroundings using state-of-art probabilistic seismic hazard analysis (PSHA) methods, at the rock level.

Seismic Background

The terrain of Delhi is flat in general except for the NNE-SSW trending ridge. This is one of the prominent features of Delhi. This is considered as an extension of the Aravalli hill, which is buried under the Yamuna alluvium in the northern parts of Delhi. River Yamuna, which is another prominent feature of Delhi, enters the city from north and flows southward with an eastern bend near Okhla. This path forms a tri-junction with the Lahore-Delhi ridge, and the Delhi-Haridwar Ridge. This region is seismically active and shows sporadic activity aligned in NNE-SSW direction, nearly perpendicular to the Himalayan arc. Proximity of Himalayan region makes Delhi susceptible to the earthquakes from Himalayan seismic sources also. The nearest point from the Main Boundary Thrust (MBT) to Delhi is around 160 km. A large number of fractures and faults are noticed in the Himalayas [Valdiya 8]. This zone is well known for its severe seismic activity. In comparison with this, the Delhi region is seismically less active. Srivastava and Somayajulu [6] have discussed the geological structures and seismicity of the target area. Their study suggests that the Sonepath-Delhi-Sohna dislocation is responsible for frequent earthquakes in and around Delhi city. The epicentral map provided by them shows the presence of a seismogenic source inside the city limits. Data on the magnitude and location of past earthquakes have been collected from different catalogues. In engineering studies, it is the usual practice to consider a region of 250-300 kms., around the site for purposes of seismio-tectonic characterization [9]. Here, with India Gate in Delhi as the center, a circular region of 300 km radius has been assumed as the catchment area for Delhi city. Tectonic features around Delhi city have been previously discussed by [8]. This has been further improved here to map all known faults in a radius of 300 km., around Delhi city. Twenty faults recognizable as affecting Delhi are shown in Figure-1. Among these, eighteen faults have been marked following the Seismo-tectonic Atlas of India [10]. A short fault within Delhi city has been identified based on a report of GSI. Sohna fault has been marked in Figure-1 based on the work of Srivastava and Roy [2]. Faults such as MBF and MCT have several parallel tributaries also. In the present study, such branches have been merged with the parent fault. Figure-2 shows all known past epicenters. This map again shows Delhi's susceptibility to earthquakes from Himalayan origin as well as from local sources. The faults are numbered for further reference and their details are presented in Table-1. The magnitude M_u given in this table refers to the maximum potential local magnitude (M_L) of a particular fault. This value of M_u has been assigned based on past information, without being overly conservative.

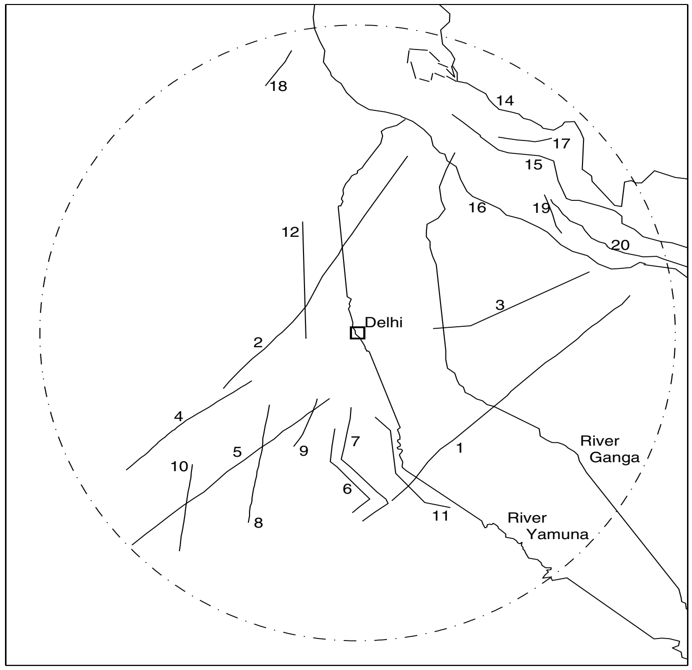

Figure 1. Fault map around Delhi City

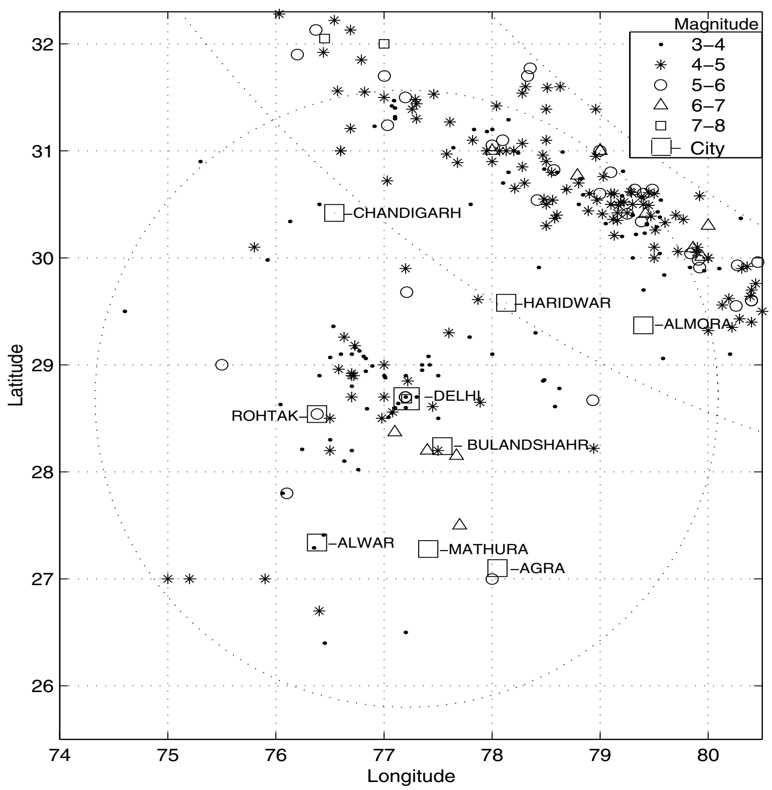

Figure 2. Epicentres of past earthquakes around Delhi

Table 1: Fault characteristics

No..	Fault Name	M_u	Length Km.	w_s
1	Great Boundary Fault (GBF)	7	320	0.1462
2	Mahendraghar-Dehradun (M-D)	7	300	0.2657
3	Moradabad	6.5	165	0.0790
4	Chahapoli	5.5	215	0.0872
5	Sabi Fracture	5.5	195	0.0796
6	Near Mathura	5	84	0.0371
7	Fault Parallel to no. 6	5.5	115	0.0490
8	Fault left of Alwar	5	130	0.0547
9	Fault near Alwar	5	55	0.0260
10	Fault near Jaipur	5	117	0.0497
11	Mathura	6	100	0.0432
12	Sohna	6	105	0.0719
13	Delhi	4.5	7	0.0106
14	Main Central Thrust (MCT)	8	350	0.5847
15	North Almora thrust (NAT)	6.9	280	0.1315
16	Main Boundary Thrust (MBT)	8	450	0.1647
17	Alaknanda	5.5	51	0.0454
18	Ropar	5	35	0.0144
19	Near Ramgarh	5	37	0.0149
20	South Almora Thrust (SAT)	6.5	130	0.0444

Regional Seismicity

The seismic hazard at Delhi is a function of the seismogenic activity of the region, which in turn will be directly related to the recurrence relationship of the listed twenty faults. This amounts to stating that if the regional seismicity can be determined, the same can be accounted for in differing proportions by the twenty faults. Here we consider the historical period to be 1720-2001, during which there were 278 catalogued events of $M_L \geq 3$ in the region. Aftershocks of large events have been omitted from this list. It is well known that catalogues contain more number of small magnitude events of recent dates detected with the help of instruments. On the other hand, larger earthquakes are rare but even without instruments their occurrence magnitude would be known from general regional history and damage data. These points to the limitation that any regional catalogue will be complete, at different magnitude levels, with differing periods of representative history. Quantification of completeness of a catalogue is essential to arrive at reliable (*a, b*) values in the Gutenberg-Richter recurrence relationship. Here, an additional complication arises due to the control region being not seismically homogenous. Since limited amount of reliable data are available, the control region has been divided into two parts denoted as the Himalayan region (HR) and the Delhi region (DR) as shown in Figure-2. The completeness of the catalogue has been investigated by the approach given by Stepp [11]. It is found that in the Delhi region for 3-4, 4-5, 5-6 and 6-7 magnitude groups the data is complete for 10, 40, 70, 290 years respectively. It is also found that in the Himalayan region for 3-4, 4-5, 5-6, 6-7, and 7-8 magnitude groups the data is complete for 10, 20, 70, 100, 100 years respectively. The completeness of different magnitude groups are shown in Table-2. It is likely that these results are not very accurate, but are the best possible estimates at present. It is taken for further work that the data set is complete above magnitude 6.0, for both the regions. In Figure-3, recurrence results obtained by Stepp's method are shown without truncation of the magnitude values at the upper end. A method proposed by Kijko [12] has also been used as an alternate approach to obtain the recurrence curves. This method uses the method of maximum likelihood to find the b value. This method can handle errors in magnitude values and incompleteness in the data set. For this analysis, here the magnitude is truncated at the upper end, as a normal random variable with mean value M_u and standard deviation 0.1 This method gives b=0.78 for the Himalayan region and b=0.87 for the Delhi region. The recurrence relationships for these two sub-regions are shown in Figure-3. For further work, the doubly truncated magnitude distribution is used since it does not exaggerate the occurrence of large magnitude earthquakes.

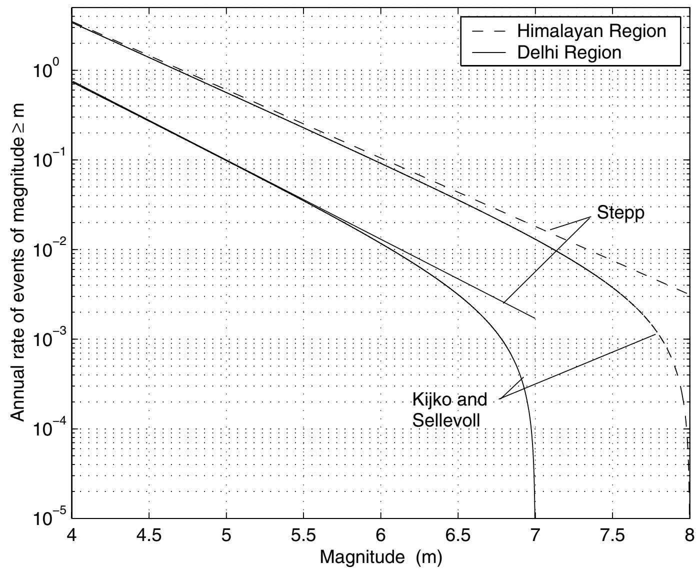

Figure 3. Regional magnitude-frequency relationship

Table 2: Completeness of different magnitude group

M_L	No. of events per year ≥ M_L	Complete (Year)	M_L	No. of events per year ≥ M_L	Complete (Year)
Delhi Region			Himalayan Region		
3	3.3879	10	3	8.3714	10
4	0.7879	40	4	4.0714	20
5	0.0741	70	5	0.4714	70
6	0.0138	290	6	0.1000	100
			7	0.0200	100

Individual Fault Recurrence

A given point in the target region will be subject to ground motion from any of the twenty faults. However, each fault has different length, orientation and seismic activity rate. To compute the ground motion due to an event on a particular fault source *s* one needs to know the magnitude of the event and the site to source distance. The magnitude of a future event on any fault is a random variable since that fault has potential to produce an earthquake of magnitude *m* in the interval (m_0, m_u) as per its own recurrence properties, which is not yet known. To circumvent this difficulty, the heuristic principle of conservation of seismic activity is used. As per this, $N_r(m_0)$, the number of earthquakes per year with $m>m_0$, in the region should be equal to the sum of individual $N_s(m_0)$ (s=1,2,…N_s) values. For PSHA m_0 can be fixed at 4.0 since events of still lower magnitudes are not of engineering importance. However, any fault with a length greater than the required rupture length at m_0=4, can generate an event in future. This observation leads one to recognize that $N_s(m_0)$ may be taken to be proportional to the length of the fault. This gives the weighting factor $\alpha_s=L_s/\sum L_s$ as an activity indicator for fault ***s***. However this need not be the only factor influencing $N_s(m_0)$. For example, a shorter fault may be more active at the lower magnitude level m_0, than a longer fault that is

capable of producing a higher magnitude. This property can be included if the slip rate of various faults in the region are known. Since for the region under consideration this is not known, we proceed differently. All the past earthquakes are assigned to the twenty faults depending on the proximity of the corresponding epicenters to these faults. This way another weighing factor δ_s, which is the ratio of the past earthquakes attributed to fault *s* to the total number of earthquakes in the region is obtained.
This leads to the relation

$$N_s(m_0) = 0.5(\alpha_s + \delta_s)\, N_r(m_0) \qquad (s=1,2,\ldots.20) \tag{1}$$

The weight w_s=0.5(α_s + δ_s) assigned to each fault is given in Table-1. The recurrence relation of each fault capable of producing earthquake magnitude in the range m_0 to m_u can be taken as

$$N^s(m) = N^s(m_0)\left[1 - \frac{1 - e^{-\beta(m - m_0)}}{1 - e^{-\beta(m_u - m_0)}}\right] \tag{2}$$

Table 3. Magnitudes corresponding to 100 years and 500 years recurrence period

Fault no.	Shortest hypocentral distance (km)	Magnitude		Fault no.	Shortest hypocentral distance(km)	Magnitude	
	R	M_{100}	M_{500}		R	M_{100}	M_{500}
1	153	5.2	5.9	11	87	4.6	5.3
2	54	5.5	6.2	12	43	4.8	5.5
3	93	4.9	5.6	13	10	3.9	4.3
4	111	4.8	5.3	14	275	6.9	7.5
5	91	4.8	5.2	15	235	6.0	6.6
6	99	4.4	4.8	16	183	6.2	7.0
7	81	4.6	5.1	17	244	5.1	5.4
8	107	4.5	4.9	18	261	4.6	4.9
9	74	4.3	4.8	19	217	4.6	4.9
10	115	4.5	4.9	20	237	5.4	6.0

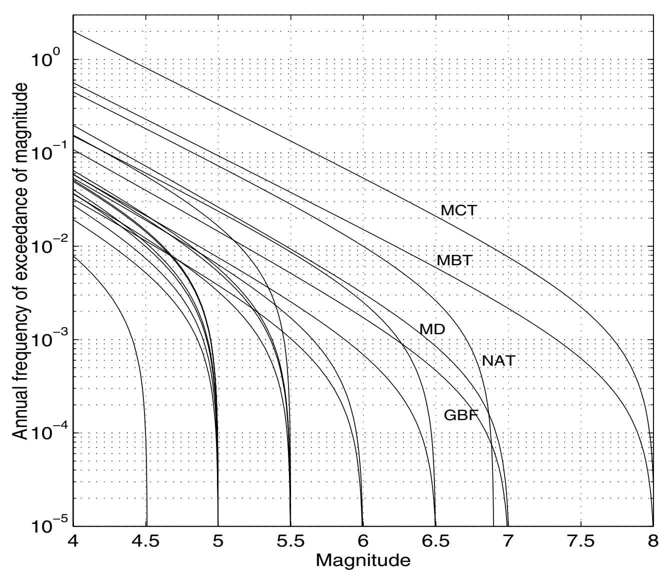

Figure 4. Deaggregation of regional hazard in terms of fault recurrence

With the help of the above expression, the regional recurrence is deaggregated into individual fault recurrence as shown in Figure-4. Here it may be mentioned that the b-value of all faults have been taken to be equal to the regional b-value. One can get from this figure the estimated magnitude of future earthquakes of particular recurrence periods occurring on any fault within the region. In deterministic hazard analysis, one proceeds to find the nearest distance from a given site to the various faults and the possible magnitudes corresponding to 100 or 500 years recurrence on the faults. With this in view, M_{100} and M_{500} for all the faults along with their shortest distance to India Gate in Delhi have been listed in Table-3. In finding R, the focal depth is assumed at an average value of 10 kms.

Magnitude Uncertainty

For a given site, even when the causative faults are known along with their (*a, b*) values, the magnitude of a possible future event remains uncertain. However, the magnitude is a random variable distributed between m_0 and m_u**.** Since, the recurrence relation is known to be of the form

$$\log_{10} N(m) = a - bm \tag{3}$$

It follows *M* will be a random variable following the probability density function, Kiureghian and Ang [13].

$$p_M(m) = \frac{\beta e^{-\beta(m-m_0)}}{1-e^{-\beta(m_u-m_0)}} \quad (m_0 \le m \le m_u) \tag{4}$$

Here β=2.303b and Here m_0 and m_u are respectively the threshold and the maximum possible magnitudes.

Uncertainty in Hypocentral Distance

Another important parameter, which is uncertain, is the source to site distance. On an active fault it is possible that all points are equally vulnerable to rupture. Thus, depending on the relative orientation of a fault with respect to the station, the hypocentral distance *R* will have to be treated as a random variable. In the present study, all faults are considered linear with known lengths in the control region (Table-1). Further following, Kiureghian and Ang [13] the conditional probability distribution function of *R* given that the magnitude *M* = *m* for a rupture segment, uniformly distributed along a fault is given by

$$P(R < r \mid M = m) = 0 \qquad \text{for } R < (D^2 + L_0^2)^{1/2}$$

$$P(R < r \mid M = m) = \frac{(r^2 - d^2)^{1/2} - L_0}{L - X(m)} \quad \text{for } (D^2 + L_0^2)^{1/2} \le R < \left\{D^2 + \left[L + L_0 - X(m)\right]^2\right\}^{1/2}$$

$$P(R < r \mid M = m) = 1 \qquad \text{for } R > \left\{D^2 + \left[L + L_0 - X(m)\right]^2\right\}^{1/2} \tag{5}$$

Here, *X(m)* the rupture length in kilometers, for an event of magnitude *m* is given by

$$X(m) = MIN\left[10^{(-2.44+0.59m)}, fault\ length\right] \tag{6}$$

The notations in the above equation are explained in Figure-5. In equation (6) *MIN* stands for the minimum of the two arguments inside the parentheses. This condition is used to confine the rupture to the fault length. The first term, provides an estimate for the rupture length expected for an event of magnitude *m* [14]. The above solution pertains to the case of a fault situated entirely to one side of a site. In a more general situation when the fault is extending on both sides of the source, the conditional probabilities for the two sides are multiplied by the fraction of length of the corresponding sides and summed up to get the probability for the total fault.

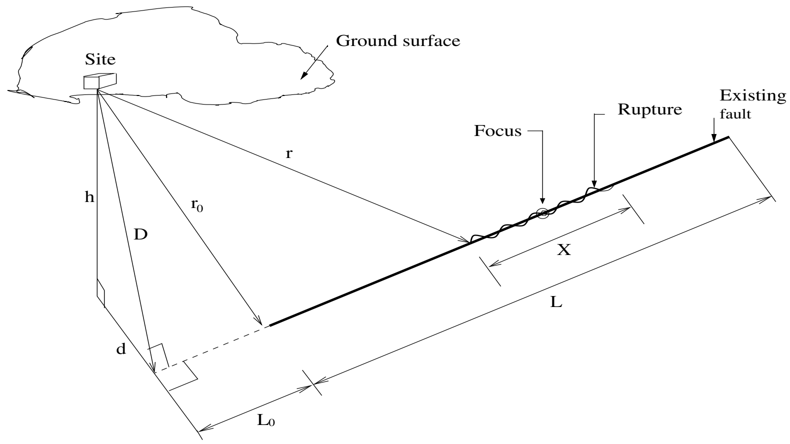

Figure 5. Fault rupture model

Attenuation

There are very few established attenuation relationships based on actual SMA data for Indian regions. Sharma [15], Jain *et al* [16], and Saini *et al* [17], have proposed general attenuation equations for the broad Himalayan region, which would encompass large areas of North India. Among the above, the study of Sharma [15] is relevant to the Delhi region. However, his study does not report the standard error in the empirical attenuation formula, making it not usable in PSHA. Further, since Delhi city is overlain with soft soil over a large area, it would be advantageous to have an attenuation relation valid specifically for rock sites. This would help engineers in using softwares such as SHAKE91 in soil amplification and liquefaction studies. Hence, a fresh effort has been made to derive an attenuation relationship for the region under consideration drawing recorded PGA data from literature. A database containing 61 data of nine earthquakes have been used. Out of these 61 values, 52 PGA values are on rock. At other sites, the soil conditions are not well known. The list of earthquakes for which the data is available and hence used here is given in Table-4. The PGA data considered are primarily from the Himalayan region, with a few additional data on rock sites from NE India and Delhi region. The database contains nine spectral response recorder (SRR) data of Uttarakashi earthquake, at seven stations on rock [18]. The SRR instruments directly give a point on the response spectrum $S_a(\eta, T_n)$ for a particular value of damping η and natural period T_n. From the SRR data, PGA values have been estimated following the work of Iyengar and Raghukanth [19]. They have derived a relation is of the form

$$\ln(PGA)=a_1+a_2\ln S_a(0.05,0.4)+a_3\ln S_a(0.05,0.75)+a_4\ln S_a(0.1,0.4)+a_5\ln S_a(0.1,0.75)+\ln\varepsilon$$

a_1= -0.5158; a_2=0.25; a_3=-0.2488; a_4=0.8586; a_5=0.2922; $\sigma_{(\log\varepsilon)}$=0.3429

The attenuation equation selected has the form proposed by Sharma [15] and Campbell [20]

$$\log_{10}(y) = c_1 + c_2 m - B\log_{10}(r + e^{c_3 m}) + \sigma_{\log_{10}\varepsilon}\, P$$

Here, ε is the error term and and $\sigma_{\log_{10}\varepsilon}$ is the standard deviation of $\log_{10}\varepsilon$. The value of *P* equals 0 for 50% and equals 1 for 16% probability of exceedance respectively. The two-step stratified regression [21] has been used to determine the coefficients of attenuation. The coefficients in the above equations are obtained as c_1= -1.5232, c_2=0.3677, c_3=0.41, B=1.0047, σ=0.2632. A comparison between the present equation and the one given by Sharma, for mean PGA value, is shown in Figure-6. The two relations are similar except for minor differences, which is attributable to diffuse site conditions used by Sharma.

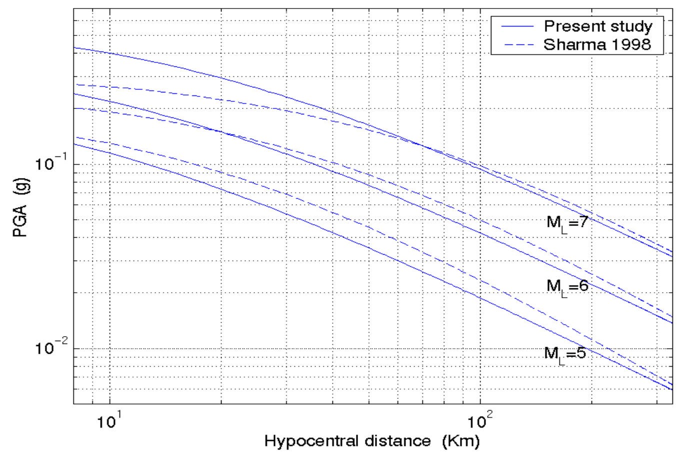

Figure 6. Attenuation of PGA in Northern India

Table 4: List of contributing earthquakes

Event No.	Date	^{0}N	^{0}E	Depth (Km)	Magnitude M_L	No. of records
2	26.04.1986	32.17	76.28	7	5.5	9
3	10.09.1986	25.42	92.08	28	5.5	7
1	21.08.1988	26.60	86.80	71	6.4	4
4	18.05.1987	25.27	94.20	50	5.7	2
5	06.02.1988	24.64	91.51	15	5.8	8
6	20.10.1991	30.73	78.79	12	6.4	19
7	29.03.1999	30.49	79.29	21	6.8	10
8	28.02.2001	28.56	76.18	35	4.0	1
9	28.04.2001	28.80	72.20	10	3.8	1

PSHA

Probabilistic seismic hazard analysis has been discussed in the literature notably by Cornell [22], Kiureghian and Ang [13] among others. Presently, leading engineering standards and manuals such as USDOE-1024, IBC-2000, USNRG-1.165 and EM-1110 of US Army Corp of Engineers, specify hazard in terms of the annual probability of exceedance of a given value. Using Poisson probability model, the probability of Y=PGA/g exceeding the level a in the design time period T at a site can be expressed in terms of the annual rate of exceedance μ_a by the equation

$$P(Y > a) = 1 - \exp(-\mu_a T) \tag{8}$$

The basic expression for μ_a is

$$\mu_a = \sum_{s=1}^{N_s} N_s(m_0) \int_m \int_r P(Y > a \mid m, r)\, p_{R|M}(r \mid m)\, p_M(m)\, dr dm \tag{9}$$

It is emphasized here that the above expression sums up all the individual contributions of twenty faults (s=1,2,…20) to obtain the annual probability of exceedance. The procedure described above is repeated systematically at different points of the city to come up with a microzonation map. Here this is achieved by dividing Delhi city region into 1200 grids of size 1km × 1km. Hazard contours representing 2% probability of exceedance in a design life of 50 years are shown in Figure-7. This corresponds to a return period of 2500 years. It is seen that due to the presence of the Delhi fault, the PGA value tends to peak at the center of the city. However, the overall hazard is governed by the Mahendragarh-Dehradun (MD) fault, as the contours are aligned along the strike direction of this fault. The south-west part of the city is controlled by the combined effect of the MD fault and the nearby Sohna fault. Figure-7, may be directly used wherever rock is exposed, or the site is classified as B-type as per NEHRP [26] classification. At other points, the effect of local soil condition has to be included before the surface level PGA value can be found.

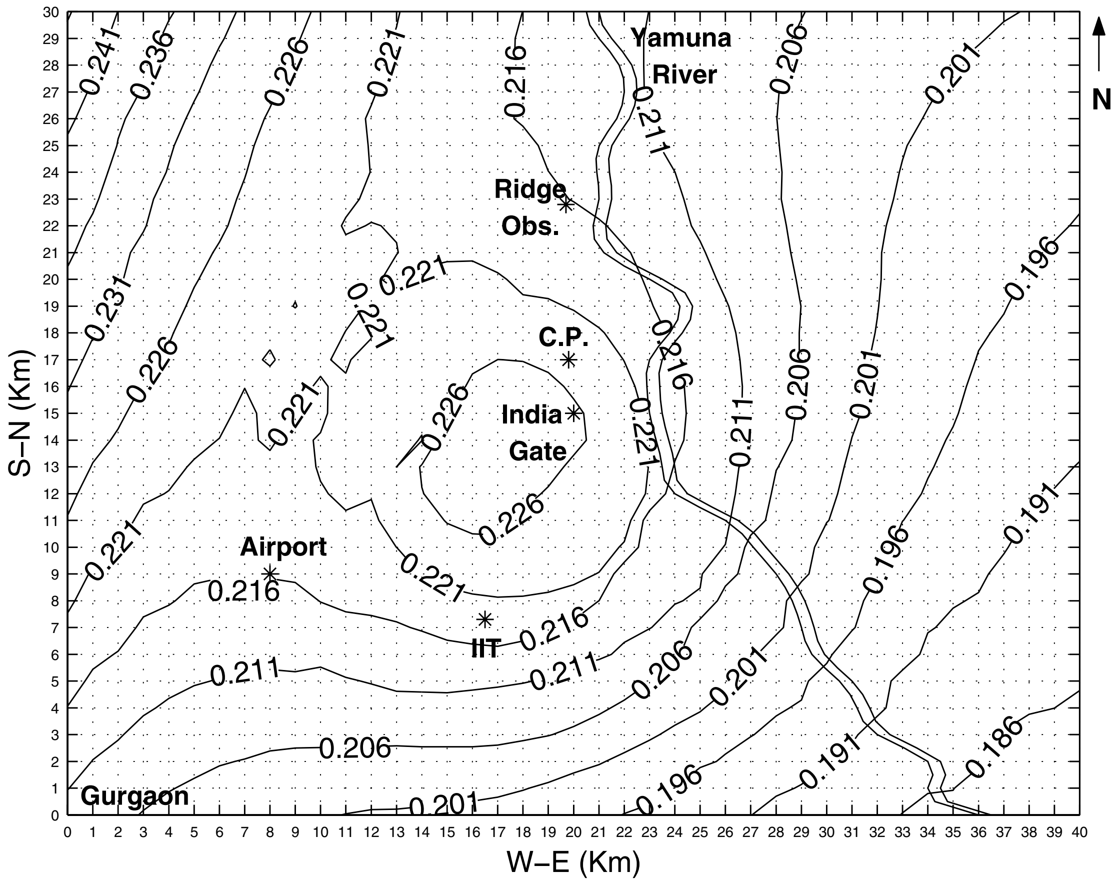

Figure 7. Microzonation Map on Bedrock. Mean PGA(g) at 2% probability of exceedance in 50 years. Return Period=2500 years.

Local site effect

Delhi exhibits surface level rock exposures in its southern suburbs. The depth of bedrock in the North Delhi area is shallow adjacent to the quartzite ridge but gradually deepens on either side of the ridge (Figure 8). As one proceeds towards River Yamuna, rock outcrops and rocky soils become infrequent and in the trans-Yamuna region rock level is very deep. The depth to bedrock below the surface increases steeply in the northeastern direction. In general, the bedrock profile is undulating with several humps and depressions overlain with soil deposits. Detailed measurements of bedrock depth profile in Delhi are not yet available. Hence, surface level PGA values have not been fully mapped in this study. Geotechnical borehole data were made available by M/S Tandon Consultants Pvt. Ltd, New Delhi, for seventeen sites. In Table-5 some details of this data with location and bedrock depth are shown. The locations of these sites are also marked on Figure-8 for easy reference. Measured shear wave velocity (V_s) data is again not known for any site in Delhi. Hence this parameter has been estimated from measured SPT values using a relationship proposed by Turnbull [23] based on Japanese data. In Figure-9 the variation of estimated V_s values with depth is shown. It is usual to express the variation of V_s with depth in terms of a power law [24,25]. With the help of about 175 samples, the parameters of regression of the equation (10) have been obtained as K=173.12, n=0.20; with standard deviation of the error equal to 41.16 m/s.

$$V_s = K\,D^n + error \tag{10}$$

One dimensional soil amplification analysis based on multiple reflection theory of vertically propagating shear waves has been performed using software SHAKE91 at the seventeen sites with available soil data. In this analysis V_s for rock has been taken as 1.5 km/s. The ratio of equivalent uniform shear strain to maximum shear strain is taken as 0.65. The modulus reduction curve and damping curve are taken from Seed [27]. Frequency response functions for all the seventeen sites have been found corresponding to unit amplitude sinusoidal excitation at rock level. Some of these results are presented in Figure-10 to show the amount of amplification possible at resonance. The resonant frequency of these seventeen sites with known soil layer properties is shown in Figure-11. In the same figure natural frequency of the soil layer modeled as a shear beam with the shear wave velocity of equation (10) is plotted as a function of depth to bedrock. It is observed that the approximate power law profile for V_s is quite accurate in predicting the site natural frequency, as compared with more elaborate computations using different layer properties. Figure 11 indicates that in Delhi beyond a depth of 150 meters the nature of the deposit may not have significant effect on the first natural frequency and hence on soil amplification. Based on the shear wave velocity profile the sites were classified according to IBC-2000 [28] guideline and reported in Table-5.

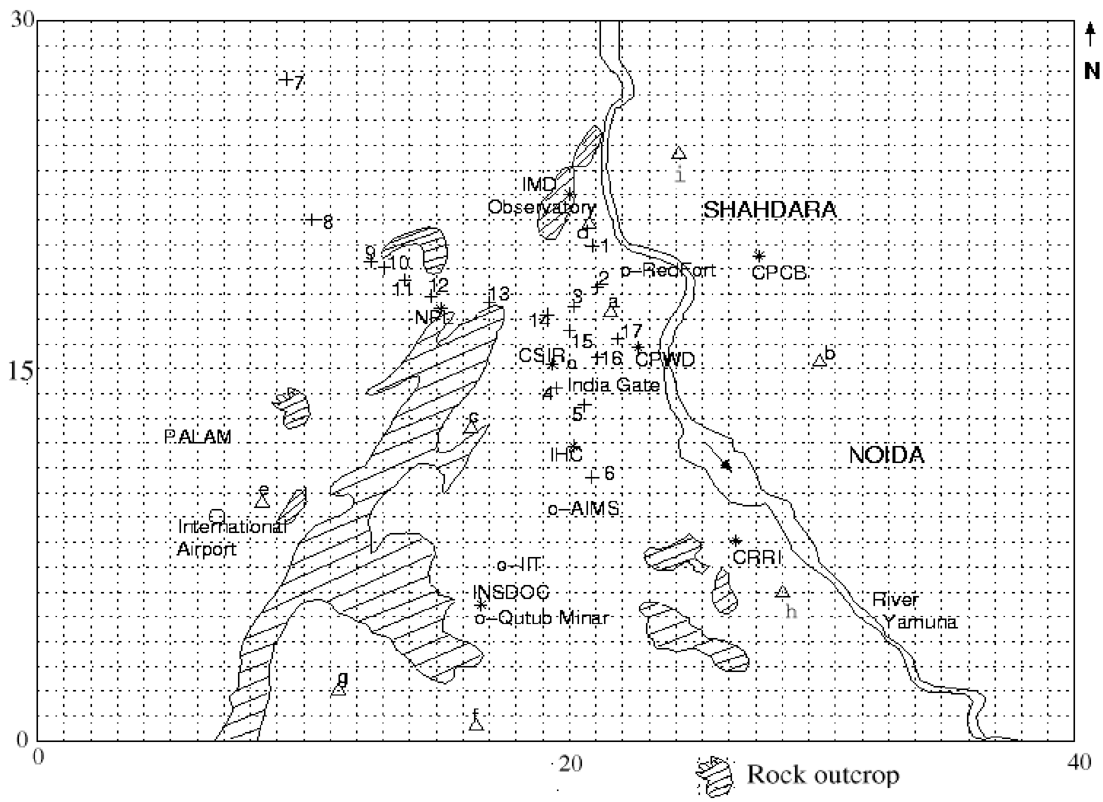

Figure 8. Rock profile of Delhi City

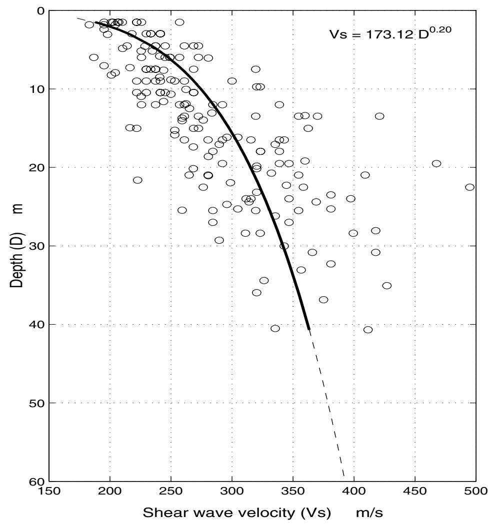

Figure 9. Approximate Shear-wave velocity profile for top soils in Delhi City

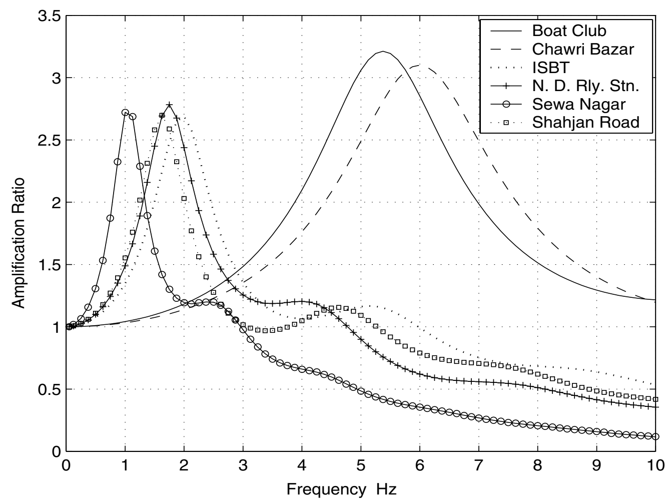

Figure 10. Frequency Response Function at sites with known layer data

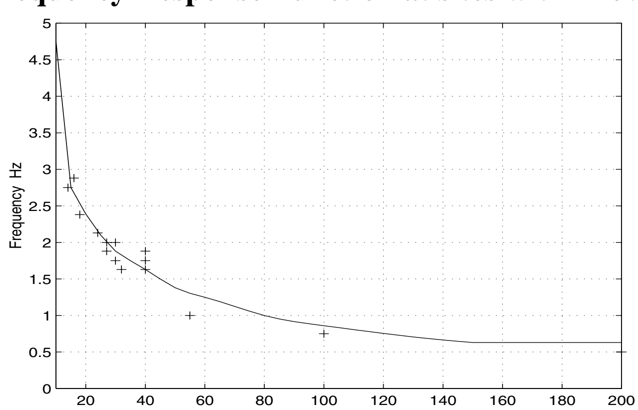

Figure 11. Variation of first natural frequency with bed-rock depth

Table 5. Site Natural Frequencies and classification

Site no. in fig. 8	Location	Grid coordinates in Fig 8 (km)	Bed-rock depth m	Nat Freq Hz	Bedrock to Surface amplification at resonance	V_s^{30} m/s	Site Class As per IBC 2000
1	Sewanagar	20.9,20.0	55	1.00	2.72	234.6	D
2	Shahjahan Road	21.0,18.0	32	1.63	2.70	269.9	D
3	Boat Club	20.1,17.5	12	5.38	3.21	1009	B
4	N.D. Rly.Stn.	19.5,14.2	30	1.75	2.78	278.6	D
5	Chawri Bazar	20.6,13.5	09	6.00	3.10	1130.2	B
6	ISBT	20.9,10.6	30	2.00	2.69	317.0	D
7	Rohini	09.3,27.7	200	0.50	2.41	269.4	D
8	Punjabi Bagh	10.3,21.0	100	0.75	2.58	271.3	D
9	Kirti Nagar & Metro Station	12.5,19.2	40	1.63	2.81	317.9	D
10	Rama Rd. and PatelRd. Junction	13.0,19.0	27	2.00	2.59	296.1	D
11	Naraina Rd. and Patel Rd. Junction	13.9,18.5	16	2.88	2.49	833.9	C
12	Patel Nagar Metro Station	14.8,18.0	14	2.74	2.40	910.4	B
13	Karol Bagh Metro Station	17.0,17.5	27	1.88	2.59	420.3	C
14	Palika Place Metro Station	19.2,17.2	24	2.13	2.55	523.9	C
15	Connaught Place	20.0,16.5	18	2.38	2.47	747.9	C
16	Mandi House	21.0,15.5	40	1.88	2.52	339.5	D
17	Tilak Bridge	22.8,16.2	40	1.75	2.74	256.6	D

Summary and Conclusion

Seismic hazard microzonation results for Delhi city are presented in this paper. After a review of the seismo-tectonic set up around Delhi, a controlling region of 300 km radius is considered for detailed study. Regional recurrence relations are obtained based on 300 years of past data. The regional seismicity is distributed among twenty faults of varying lengths and potential. An attenuation relationship valid for the region based on instrumental data on hard rock sites has been derived. Probabilistic seismic hazard analysis has been carried out to arrive at the mean annual probability of exceedance of PGA value at any site in Delhi city. Detailed results are presented in the form of a contour map covering Delhi city and its environs on a grid of 1km x 1km. Engineers can use this map directly for hard rock sites (B-type) in Delhi. However, for other sites further amplification factors are to be found to arrive at surface level PGA values. Here some limited site effect studies have been carried out. From the limited amount of borehole data so far collected, it is clear that there are severe variations in the depth to bedrock. This can cause considerable spatial variation in the surface level ground motion. The first natural frequency presented in Table-5, shows that sites with thick soil deposits, like in Sewanagar, Rohini and Punjabi Bagh have lower natural frequencies than other sites where the thickness is less. The magnification factor corresponding to resonance at different sites suggests that the amplification factor due to soil deposits can be of the order of 2.5-3.0. Hence, the basic design PGA value in the trans-Yamuna region of Delhi with deep soil deposits will be higher than 0.24 g. The microzonation map given here can be used as the basis for further studies on site effects, with locally measured engineering properties of soils.

REFERENCES

1. Chauhan RKS. “Seismotectonics of Delhi Region”. Proceedings INSA 1975; 41: 429-447.

2. Srivastava VK, Roy AK. “Seismotectonics and seismic risk study in and around Delhi region”. Proceedings, IV Congress International Association of Engineering Geology, New Delhi, 1982; III: 77-86

3. Iyengar RN. “Seismic Status of Delhi Megacity”. Current Science, 2000; 78(5): 568-574.

4. Iyengar RN, Ghosh S. “Seismic hazard microzonation of Delhi city”. National conference on disaster management and mitigation, Chennai, Indian National Academy of Engineering, 2003: 93-108.

5. Verma RK, Roonwal GS, Kamble VP, Mohanty WK. “Seismicity of Delhi and its surrounding region”. Himalayan Geology, 1995; 6: 75-82.

6. Srivastava LS, Somayajulu JG. “The seismicity of the area around Delhi”. Proceedings of the 3rd Symposium on Earthquake Engineering, Roorkee, 1966; 1: 417-422.

7. India Meterological Department (IMD), Govt. of India. “Chamoli Earthquake of March 29, 1999 and Its Aftershocks”. New Delhi, January 2000.

8. Valdiya KS. “Himalayan transverse faults and folds and their parallelism with subsurface structures of north Indian plains”. Tectonophysics, 1976; 32: 353-386.

9. U.S. Nuclear Regulatory Commission, “Regulatory Guide 1.165; Identification and characterization of seismic sources and determination of safe shut down (SSE) ground motion”. U.S. Nuclear Regulatory Commission, Office of Nuclear Regulatory Research, Washington, USNRC (1997), Regulatory Guide DG-1032 (RG 1.165), 1997.

10. Geological Survey of India, Dasgupta S *et al.* “Seismotectonic Atlas of India and Its Environs”. 2000.

11. Stepp JC. “Analysis of Completeness of the Earthquake Sample in the Puget Sound Area and Its Effect on Statistical Estimates of Earthquake Hazard”. Microzonation Conference, Proceedings of the International Conference on Microzonation for Safer Construction Research and Application, National Science Foundation, *et al.*, Seattle Oct. 1972; II :897-909.

12. Kijko A, Sellevoll MA. “Estimation of Earthquake Hazard Parameters from Incomplete Data Files. Part II: Incorporation of Magnitude Heterogeneity”. Bulletin of the Seismological Society of America, 1992; (82):120-134.

13. Kiureghian Der A, Ang A HS. “A fault rupture model for seismic risk analysis”. Bulletin of the Seismological Society of America, 1977; 67(4): 1173-1194.

14. Wells DL, Coppersmith KJ. “New empirical relationships among magnitude, rupture length, rupture width, rupture area, and surface displacement”, Bulletin of the Seismological Society of America, 1994; 84(4): 974-1002.

15. Sharma ML. “Attenuation relationship for estimation of peak ground acceleration using data from strong-motion arrays in India”. Bulletin of the Seismological Society of America, 1998; 88(4): 1063-1069.

16. Jain SK, Roshan AD, Arlekar JN, Basu PC. “Empirical attenuation relationships for the Himalayan earthquakes based on Indian strong-motion data”, Proceedings of the 6th International Conference on Seismic Zonation, 12-15 November, Palm Spring, CA, USA, 2000,

17. Saini S, Sharma ML, Mukhopadhay S. “Strong ground motion empirical attenuation relationship for seismic hazard estimation in Himalayan region”, 12th Symposium on Earthquake Engineering, IIT Roorkee, India, pp. 143-150, 2002.

18. Department of Earthuake Engineering, University of Roorkee, “Performance of strong motion instruments in Garwal (UP) earthquake of october 20, 1991, Volume I Analysis of records obtained on structural response recorders”. Department of Earthuake Engineering, University of Roorkee, India, 1993.

19. Iyengar RN, Raghukanth STG. “Attenuation of strong ground motion in Peninsular India”. Seismological Research Letters, under review,

20. Campbell, K.W. “Near source attenuation for peak horizontal acceleration”. Bulletin of the Seismological Society of America, 1981; 71(6): 2039-2070.

21. Joyner WB, Boore DM. “Peak horizontal acceleration and velocity from strong motion records from the 1979 Imperial Vally, California, Earthquake” Bulletin of the Seismological Society of America, 1981; 71(6): 2011-2038.

22. Cornell C Allen. “Engineeing seismic risk analysis”. Bulletin of the Seismological Society of America, 1968; 58(5): 1503-1606.

23. Turnbull ML. “Seismic Hazard Assessment and Microzonation of Bundaberg”. Master's Thesis, Faculty of Engineering and Physical Systems, Central Queensland bounded University, 2001.

24. Lew M, Campbell KW. “Relationships between shear wave velocity and depth of overburden; Measurement and use of shear wave velocity for evaluating dynamic soil properties”, American Society of Civil Engineers, New York, May, 1985.

25. Lachet C, Hatzfeld D, Bard PY, Theodulidis N, Papaioannou C, Savvaidis A. “Site effects and microzonation in the city of Thessaloniki Greece : comparison of different aproaches”, Bulletin of the Seismological Society of America, 1996; 86: 1692-1703.

26. Building Seismic Safety Council (BSSC) (1998). “1997 Edition NEHRP Recommended Provisions for Seismic Regulations for New Buildings and Other Structures, FEMA 302/303”. Part 1 (Provisions) and Part 2 (Commentary), developed for the Federal Emergency Management Agency, Washington, DC, 337

27. Idriss IM, Sun JI, “User's Manual for SHAKE91, A computer Program for Conducting Equivalent Linear Seismic Response Analyses of Horizontally Layered Soil Deposits”. 1992.

28. International Code Council, ICC. “International Building Code". IBC-2000.